



UNIDIMENSIONAL NUMERICAL SOLUTION ERROR ESTIMATION FOR CONVERGENT APPARENT ORDER

Carlos Henrique Marchi

Department of Mechanical Engineering, Federal University of Paraná, Curitiba, Paraná, Brazil

Antônio Fábio Carvalho da Silva

Department of Mechanical Engineering, Federal University of Santa Catarina, Florianópolis, Santa Catarina, Brazil

Numerical solutions of eight differential equations in fluid dynamics are obtained by the finite-difference method with uniform unidimensional grids and with six types of numerical approximations. The main purpose of this work is to calculate uncertainties of numerical solutions using the Richardson error estimator and another estimator which is introduced in this work. These estimators are examined for reliability and accuracy of the uncertainty for the situation in which the size of the grid elements is small. In this case, as is shown in this work, two values of uncertainty can be found that bound the discretization error.

INTRODUCTION

The error (E) in a numerical solution of a variable of interest can be expressed as [1]

$$E(\phi) = \Phi - \phi \quad (1)$$

where Φ is the exact analytical solution and ϕ is the numerical solution. Numerical solution errors in fluid dynamics are discussed in [2–11], where the process that quantifies these errors is called verification. The numerical error sources can be classified into four types: truncation errors, iteration errors, round-off errors, and programming errors.

Truncation error arises from numerical approximations which are made in the discretization of a mathematical model [4, 6, 11]. Roughly, this error decreases as the grid spacing (h) is diminished, where h is shown in Figure 1. The iteration error is the difference between the exact and the iterative solutions of the discretized

Received 15 January 2002; accepted 7 March 2002.

The first author would like to thank the sponsors who supported this work: Federal University of Paraná (UFPR), Coordenação de Aperfeiçoamento de Pessoal de Nível Superior (CAPES), Programa de Pós-Graduação em Engenharia Mecânica/Federal University of Santa Catarina (POSMEC/UFSC), and Computational Fluid Dynamics Laboratory/Federal University of Santa Catarina (SINMEC/UFSC).

Address correspondence to Carlos Henrique Marchi, Department of Mechanical Engineering, Federal University of Paraná, P. O. Box 19011, 81531-990, Curitiba, PR, Brazil. E-mail: marchi@demec.ufpr.br

NOMENCLATURE

c	coefficients in the truncation error equation	$\lambda_{\text{DDS-2}}^i$	numerical approximation of Λ^i by two-point downstream difference
C	coefficients in the discretization error equation	λ_{UDS}^i	numerical approximation of Λ^i by one-point upstream difference
E	discretization error of the numerical solution	$\lambda_{\text{CDS}}^{ii}$	numerical approximation of Λ^{ii} by central difference
h	grid spacing or distance between two successive grid points	Λ	exact analytical solution of the dependent variable
K	coefficients in the numerical solution uncertainty equation	Λ_m	exact analytical solution of the average of Λ
L	length of the problem domain	Λ^i	exact analytical solution of the first derivative of Λ
p_L	asymptotic order of the error	Λ^{ii}	exact analytical solution of the second derivative of Λ
p_U	apparent order of the uncertainty	ϕ	numerical solution of the variable of interest
p_V	true orders of the error	ϕ_C	convergent numerical solution
q	grid refinement ratio	ϕ_∞	estimated analytical solution
R_∞	Richardson series	Φ	exact analytical solution of the variable of interest
U	uncertainty or estimated error of the numerical solution	Ψ	convergence ratio
U_C	uncertainty of the numerical solution by the convergent estimator		
U_{Ri}	uncertainty of the numerical solution by the Richardson estimator		
x	spatial coordinate		
ε	truncation error		
λ	numerical solution of the dependent variable		
λ_m	numerical solution of the average of Λ		
λ_{CDS}^i	numerical approximation of Λ^i by central difference		
λ_{DDS}^i	numerical approximation of Λ^i by one-point downstream difference		

Subscripts

CDS	central differencing scheme
DDS	downstream differencing scheme
j	number of a grid node
$j - 1$	left node to the node j
$j + 1$	right node to the node j
UDS	upwind differencing scheme
1	fine grid
2	coarse grid
3	supercoarse grid

equation [11]. Grossly, this error decreases as the number of iterations is increased. The round-off error is due mainly to a finite number of digits in the arithmetic computations [12, 13]. Roughly, this error increases as the grid spacing is diminished. Programming errors include the errors caused by people in the implementation and use of a code.

The acceptable value of a numerical error depends on among other factors, the intended use of the numerical solution, budgetary constraints, available time to

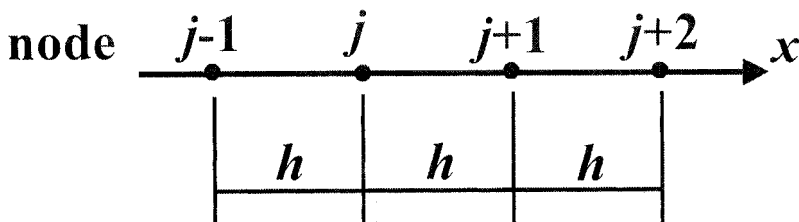


Figure 1. A uniform and unidimensional grid.

perform simulations, and available computations resources. One knows that all numerical solutions contain errors. Therefore, it is important to estimate them because of the following motives: (1) when the error is larger than the acceptable one, the numerical solution has no reliability; (2) when the error is smaller than the acceptable one, there is wasting of computational resources, that is, CPU time and memory quantity; (3) in order to validate and to develop mathematical models, for instance, turbulent flows; and (4) to optimize the grid.

In this work, it is considered that the numerical solutions do not contain iteration, round-off, or programming errors. In other words, one assumes that the numerical error defined in Eq. (1) is caused only by truncation error. In this case, it is called discretization error [6], which is also calculated by Eq. (1). Hence, its value can only be obtained as the exact analytical solution (Φ) is known. However, in practical cases, that is, when Φ is unknown, the discretization error cannot be calculated. So, the concept of uncertainty (U) is used. The uncertainty [5] of a numerical solution is defined by

$$U(\phi) = \phi_{\infty} - \phi \quad (2)$$

where ϕ_{∞} is the estimated analytical solution of a variable of interest. The uncertainty is calculated by error estimators that can be divided into two sets. In the first, the uncertainty is based on a numerical solution obtained on one grid. In general, uncertainties calculated for numerical solutions achieved by the finite-element method are in this set, as one can see in the literature [14–16]. In the second set, the uncertainty is based on numerical solutions obtained on two or more grids with different values of h . Uncertainties calculated for numerical solutions achieved by the finite-difference method and by the finite-volume method commonly are in this second set of error estimators. Examples can be seen in [2, 17], where the Richardson error estimator was used [18].

The Richardson error estimator is also used in this work. It is based on: (1) the difference between two numerical solutions obtained on two grids; (2) the grid refinement ratio; and (3) the error order. This order can be either the asymptotic (p_L) or the apparent (p_U) one. The asymptotic order [3] depends on numerical approximations used in the discretization of a mathematical model. The apparent order [19] depends on values of numerical solutions achieved on three different grids. It is recommended [7] to use the Richardson estimator only as $p_U \approx p_L$. However, in general, the values of p_U and p_L are very different from each other for grid spacings commonly used. For example, with the numerical solutions of [2, 17, 19, 20] one obtains values for the apparent order which are larger or smaller than the asymptotic order, negative values, or otherwise nonexistent values. The consequences of these differences between values of p_U and p_L have not been given suitable attention. In this work it is shown that the value of p_U and its function of h are of utmost importance in order to estimate discretization errors with accuracy and reliability. Moreover, it is shown that $p_U \approx p_L$ sometimes results in error estimates based on the Richardson extrapolation which are inaccurate and unreliable. Furthermore, it is shown that only positive apparent order values must be employed in the Richardson extrapolation.

The purpose of this work is to analyze the estimate of discretization errors in the situation where the apparent order [19] of the uncertainty converges mono-

tonically toward the asymptotic order [3] of the error. This work is developed assuming: the finite-difference method [6]; steady-state unidimensional problems with one dependent variable; uniform grids, Figure 1, that is, the grid spacing (h) is a constant in every grid; *a posteriori* error estimation [21], which can be applied to dependent variables or to variables achieved by differentiation or integration of dependent variables; and the Richardson extrapolation [3] for diminishing and estimating discretization errors.

In the following sections, the mathematical models, the types of variables, the numerical approximations, and their truncation errors used in this work are presented. Expressions are deduced for the Richardson extrapolation and the Richardson uncertainty. The concepts of Richardson series, of convergent interval of the apparent order, and of the convergent error estimator are introduced. Upper and lower bounds on analytical solutions and on discretization errors are deduced. Finally, the results and the conclusion of the work are presented.

MATHEMATICAL MODELS

The mathematical models used in this work are presented in Table 1. They model basic problems of heat transfer and fluid mechanics. Dirichlet boundary conditions [6] are used for the dependent variable (Λ). S is a constant, V is the fluid velocity, Pe is the Péclet number, and x is the independent variable. These mathematical models are linear and nonlinear, and unidimensional.

All the mathematical models have exact, continuous, unique, and known analytical solutions for each variable of interest. Therefore, it is possible to evaluate whether error estimates of numerical solutions are accurate and reliable. One defines an error estimate as accurate when the ratio between uncertainty (U) and error (E) is close to the unity. When this ratio is larger or equal to unity, the error estimate is reliable. The variables of interest are defined in the following section.

VARIABLES OF INTEREST

The exact analytical solution of every variable of interest is denoted by Φ , and the numerical solution by ϕ . Numerical solution error estimates are obtained for

Table 1. Mathematical models employed in the work

Case	Differential equation	Numerical approximations used in the differential equation
1	$V \frac{d\Delta}{dx} = 2x$	λ_{UDS}^i
2	$V \frac{d\Delta}{dx} = S$	λ_{UDS}^i
3 and 6	$V \frac{d\Delta}{dx} = 3x^2$	case 3: λ_{UDS}^i ; case 6: λ_{CDS}^i
4	$\frac{d\Delta}{dx} = \Lambda + 2x - x^2$	λ_{UDS}^i
5	$\Lambda \frac{d\Delta}{dx} = 2x^3$	λ_{UDS}^i
7	$\frac{d^2\Delta}{dx^2} = 12x^2$	λ_{CDS}^{ii}
8	$\frac{d}{dx} \left(e^\Lambda \frac{d\Delta}{dx} \right) = 0$	λ_{CDS}^i
9 and 10	$Pe \frac{d\Delta}{dx} = \frac{d^2\Delta}{dx^2}$	case 9: λ_{UDS}^i and λ_{CDS}^{ii} case 10: λ_{CDS}^i and λ_{CDS}^{ii}

Table 2. Definitions of the variables of interest

Type of variable	Analytical solution (Φ)	Numerical solution (ϕ)	Type of variable with respect to the independent variable (x)
Dependent	Λ	λ	Local
Average of the dependent variable	Λ_m	λ_m	Global
First derivative of the dependent variable	Λ^i	λ_{DDS}^i $\lambda_{\text{DDS-2}}^i$	Local

three types of variables that are shown in Table 2. The first type is the dependent variable of the mathematical models. Its exact analytical solution is denoted by Λ and its numerical solution by λ . For example, in meteorological studies, it is of interest to solve the temperature on all points of the domain.

The second type is the integral or the average of the dependent variable on the whole problem domain. Its exact analytical solution is denoted by Λ_m and its numerical solution by λ_m . In general applications, this type of variable is used to calculate mass fluxes, for example.

The third type is the derivative of the dependent variable on the left boundary of the domain, that is, at $x = 0$. Its exact analytical solution is denoted by Λ^i and its numerical solutions are denoted by λ_{DDS}^i and $\lambda_{\text{DDS-2}}^i$. In general applications, this type of variable is used, for example, to calculate heat fluxes and shear stresses.

The variable Λ , λ , Λ^i , λ_{DDS}^i , and $\lambda_{\text{DDS-2}}^i$ can be called local variables because their values depend on x . The variables Λ_m and λ_m can be called global variables because their values represent the whole problem domain.

NUMERICAL APPROXIMATIONS AND THEIR TRUNCATION ERRORS

Numerical solutions are obtained by a numerical approximation of each term of the mathematical models in Table 1. Some ways to do these approximations and the generic expressions of their truncation errors are presented in this section. Also, the concepts of true and asymptotic orders are defined.

Table 3 shows three types of variables, for which are presented six types of numerical approximations used in this work and the symbols employed to denote the analytical (Φ) and numerical (ϕ) solutions. The first variable is the first derivative of the dependent variable. Its analytical solution is denoted by Λ^i . The numerical approximations are made in four ways that are denoted by λ_{UDS}^i , λ_{CDS}^i , λ_{DDS}^i , and $\lambda_{\text{DDS-2}}^i$. The second variable is the second derivative of the dependent variable. Its analytical solution is denoted by Λ^{ii} and the numerical approximation by $\lambda_{\text{CDS}}^{ii}$. The third variable is the average of the dependent variable on the whole problem domain. Its analytical solution is denoted by Λ_m and the numerical approximation by λ_m .

For each variable of interest, the truncation error (ε) can be defined as the difference between its exact value (Φ) and its numerically approximated value (ϕ), that is,

$$\varepsilon(\phi) = \Phi - \phi \tag{3}$$

Table 3. Definitions of the numerical approximations used in the work

Type of variable	Analytical solution (Φ)	Numerical solution (ϕ)	Type of numerical approximation
First derivative of the dependent variable	Λ^i	λ_{UDS}^i	One-point upstream
		λ_{CDS}^i	Central difference
		λ_{DDS}^i	One-point downstream
		λ_{DPS-2}^i	Two-point downstream
Second derivative of the dependent variable	Λ^{ii}	λ_{CDS}^{ii}	Central difference
Average of the dependent variable	Λ_m	λ_m	Trapezoidal rule

where it is assumed that ϕ does not contain iteration, round-off, or programming errors. If the Φ and ϕ values are known, ε can be calculated by two ways. The first way is to calculate it using Eq. (3). The second way is by introducing in Eq. (3) an expression for the exact analytical solution (Φ) of the variable of interest obtained from the Taylor series and an expression for the numerical approximation (ϕ). In this case, one gets [3]

$$\varepsilon(\phi) = c_1 h^{p_L} + c_2 h^{p_2} + c_3 h^{p_3} + c_4 h^{p_4} + \dots \tag{4}$$

where the coefficients c_i can be positive or negative. These coefficients can also be functions of the dependent variable (Λ) and of its derivatives; that is, they can change with x but do not change with grid spacing (h). The exponents of h in Eq. (4) are connected to the concepts of true and asymptotic orders of the truncation error, which are defined as follows.

True and Asymptotic Orders of the Truncation Error

The true orders (p_V) are defined as the exponents of h of the nonzero terms in the truncation error equation, Eq. (4) that is, p_L, p_2, p_3, p_4 , etc. The true orders follow the relation $p_L < p_2 < p_3 < p_4$ etc., and are positive integer numbers. In general, they constitute an arithmetic progression, in other words, the difference between successive orders is a constant. Usually, the number of true orders is infinite because the truncation error equation, Eq. (4), is constituted by an infinite quantity of nonzero terms.

The smallest exponent of h in Eq. (4) is defined as the asymptotic order (p_L). It is a positive integer number and $p_L \geq 1$. As $h \rightarrow 0$, the first term of Eq. (4) is the leading term. So, p_L is the slope of an ε -versus- h logarithmic curve and indicates how fast the error is reduced as the grid spacing is reduced.

Numerical Approximations

Numerical approximations and their truncation errors can be obtained from the Taylor series, which is an infinite series and is defined by [1]

$$\Lambda_x = \sum_{n=0}^{\infty} \Lambda_j^n \frac{(x - x_j)^n}{n!} \tag{5}$$

where Λ is the dependent variable of the mathematical models, Λ_x is the exact analytical value obtained at coordinate x with a Taylor series expansion from the node j , where the exact analytical value of Λ_j and its derivatives ($\Lambda_j^i, \Lambda_j^{ii}, \dots, \Lambda_j^n$) are known. Equation (5) is valid if Λ is a continuous function of x in the closed interval $[x, x_j]$ and there are continuous derivatives up to the order n in this same interval.

Applying Eq. (5) to the nodes $j - 1$ and $j + 1$ on the uniform grid shown in Figure 1, one obtains

$$\Lambda_{j-1} = \Lambda_j - \Lambda_j^i h + \Lambda_j^{ii} \frac{h^2}{2} - \Lambda_j^{iii} \frac{h^3}{6} + \dots \tag{6}$$

$$\Lambda_{j+1} = \Lambda_j + \Lambda_j^i h + \Lambda_j^{ii} \frac{h^2}{2} + \Lambda_j^{iii} \frac{h^3}{6} + \dots \tag{7}$$

where j is a generic node used to make the numerical approximations; the three points indicate an infinite series; and h is the grid spacing, given by

$$h = x_j - x_{j-1} \tag{8}$$

Numerical approximations for the variables Λ^i, Λ^{ii} , and Λ_m given in Table 3 and others are presented, for example, in Fletcher [22], Ferziger and Peric [11], and Tannehill et al. [6]. Those use in this work are shown below.

Subtracting Eq. (6) from Eq. (7), one gets an exact analytical expression for the first derivative of the dependent variable at node j in the following form:

$$\Lambda_j^i = \frac{(\Lambda_{j+1} - \Lambda_{j-1})}{2h} - \Lambda_j^{iii} \frac{h^2}{6} - \Lambda_j^v \frac{h^4}{120} - \Lambda_j^{vii} \frac{h^6}{5,040} - \dots \tag{9}$$

where $\Lambda_j^{iii}, \Lambda_j^v$, and Λ_j^{vii} are, respectively, the third, fifth, and seventh derivatives of the dependent variable at node j . Equation (9) can be rewritten as

$$\Lambda_j^i = (\lambda_{CDS}^i)_j + \varepsilon(\lambda_{CDS}^i)_j \tag{10}$$

where the first term on the right-hand side of Eq. (9) is the numerical approximation by central difference for the first derivative, that is,

$$(\lambda_{CDS}^i)_j = \frac{(\Lambda_{j+1} - \Lambda_{j-1})}{2h} \tag{11}$$

and the remaining terms in Eq. (9) are the truncation error of λ_{CDS}^i , given by

$$\varepsilon(\lambda_{CDS}^i)_j = -\Lambda_j^{iii} \frac{h^2}{6} - \Lambda_j^v \frac{h^4}{120} - \Lambda_j^{vii} \frac{h^6}{5,040} - \dots \tag{12}$$

Comparing Eq. (4) to Eq. (12), it can be observed that the true orders of $\varepsilon(\lambda_{CDS}^i)$ are $p_V = 2, 4, 6$, etc., and, then, its asymptotic order is $p_L = 2$. So, one says that the truncation error of λ_{CDS}^i is of second order. Furthermore, $c_1 = -\Lambda_j^{iii}/6$, $c_2 = -\Lambda_j^v/120$, $c_3 = -\Lambda_j^{vii}/5,040$, etc., that is, the coefficients c_i are functions of x and of derivatives of the dependent variable.

In a similar way used to achieve Eq. (11), numerical approximations for the first derivative by one-point upstream, one-point downstream, and two-point downstream are given, respectively, by

$$(\lambda_{UDS}^i)_j = \frac{(\Lambda_j - \Lambda_{j-1})}{h} \tag{13}$$

$$(\lambda_{DDS}^i)_j = \frac{(\Lambda_{j+1} - \Lambda_j)}{h} \tag{14}$$

$$(\lambda_{DDS-2}^i)_j = \frac{(4\Lambda_{j+1} - 3\Lambda_j - \Lambda_{j+2})}{2h} \tag{15}$$

The numerical approximation by central difference for the second derivative results in

$$(\lambda_{CDS}^{ii})_j = \frac{(\Lambda_{j-1} + \Lambda_{j+1} - 2\Lambda_j)}{h^2} \tag{16}$$

The exact analytical solution of the averaged dependent variable on the whole problem domain is calculated by

$$\Lambda_m = \frac{I}{L} \int_0^L \Lambda \, dx \tag{17}$$

where L is the length of the whole problem domain. The numerical approximation for Λ_m , obtained by the trapezoidal rule [23], is given by

$$\lambda_m = \frac{h}{2L} \sum_{j=1}^N (\Lambda_{j-1} + \Lambda_j) \tag{18}$$

where N is the number of grid elements. Table 4 shows a summary of the true and asymptotic orders of the truncation errors expected for the six numerical approximations presented in this section.

THE RICHARDSON ERROR ESTIMATOR

The discretization error can be calculated by Eq. (1). It can also be calculated assuming an analogy [4, 11, 24] to the truncation error equation, Eq. (4), that is,

Table 4. Expected values for the orders of the truncation errors

Numerical solution (ϕ)	Type of numerical approximation	True orders (p_V)	Asymptotic order (p_L)
λ_{UDS}^i	One-point upstream	1, 2, 3, ...	1
λ_{CDS}^i	Central difference	2, 4, 6, ...	2
λ_{DDS}^i	One-point downstream	1, 2, 3, ...	1
λ_{DDS-2}^i	Two-point downstream	2, 3, 4, ...	2
λ_{CDS}^{ii}	Central difference	2, 4, 6, ...	2
λ_m	Trapezoidal rule	2, 4, 6, ...	2

$$E(\phi) = C_1 h^{p_L} + C_2 h^{p_2} + C_3 h^{p_3} + C_4 h^{p_4} + \dots \quad (19)$$

where the coefficients C_i can be equal to or different from the coefficients c_i in Eq. (4). They can be positive or negative and can be functions of the dependent variable (Λ) and of its derivatives; that is, they can change with x but it is assumed that they are independent of the grid spacing (h). In the same form as Eq. (4), one can define true and asymptotic orders in Eq. (19) whose definitions are equal to those in the previous section.

The value of the discretization error can only be calculated by Eq. (1) or by Eq. (19) when the exact analytical solution is known. When it is unknown, the concept of uncertainty defined in Eq. (2) is used. The uncertainty can be obtained, for example, by the Richardson error estimator [2, 18]. According to it, the uncertainty (U_{Ri}) of a numerical solution (ϕ) is given by

$$U_{Ri}(\phi) = \phi_\infty - \phi \quad (20)$$

where ϕ represents the numerical solution of each variable of interest in Table 2, and ϕ_∞ denotes the estimated analytical solution. The value of ϕ_∞ is obtained by the Richardson extrapolation [3, 18, 24] as

$$\phi_\infty = \phi_1 + \frac{(\phi_1 - \phi_2)}{(q^{p_L} - 1)} \quad (21)$$

where ϕ_1 and ϕ_2 are numerical solutions obtained on fine (h_1) and coarse (h_2) grids, respectively; p_L is the asymptotic order of the discretization error; and q is the grid refinement ratio defined by

$$q = \frac{h_2}{h_1} \quad (22)$$

Introducing Eq. (21) into Eq. (20), the Richardson error estimator results in

$$U_{Ri}(\phi_1) = \frac{(\phi_1 - \phi_2)}{(q^{p_L} - 1)} \quad (23)$$

In order to get a reliable uncertainty calculated by the Richardson error estimator it is necessary to have $U_{Ri}/E \geq 1$, that is, the analytical solution (Φ) may be between ϕ_1 and ϕ_∞ . Figure 2 illustrates a reliable uncertainty (U_{Ri}) that was obtained by the Richardson error estimator. The values of U_{Ri} and ϕ_∞ , given by Eqs. (23) and (21), respectively, are exactly equal to the discretization error (E) and to the exact analytical solution (Φ) in the particular case when the discretization error equation, Eq. (19), is constituted by a single term, as follows.

Deduction of the Richardson Extrapolation with Asymptotic Order

The expression of the Richardson extrapolation, Eq. (21), is obtained [3] assuming that the uncertainty (U) of a numerical solution (ϕ) is given by

$$U(\phi) = K_U h^{p_L} \quad (24)$$

where K_U is a coefficient which is assumed has a constant value, that is, it does not change with h ; h is the grid spacing; and p_L is the asymptotic order of the

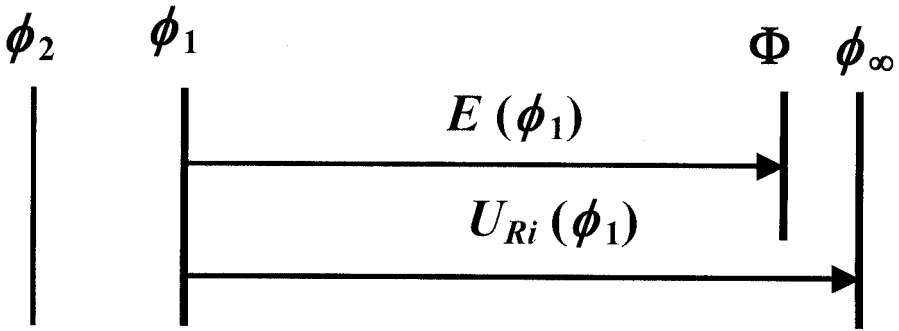


Figure 2. Example of a reliable uncertainty (U_{Ri}) obtained by the Richardson error estimator.

discretization error. With Eq. (24) applied to two different grids, h_1 and h_2 , whose numerical solutions are ϕ_1 and ϕ_2 , respectively, one gets

$$U(\phi_1) = K_U h_1^{p_L} \tag{25}$$

$$U(\phi_2) = K_U h_2^{p_L} \tag{26}$$

Introducing Eq. (20) into Eqs. (25) and (26), one obtains

$$\phi_\infty - \phi_1 = K_U h_1^{p_L} \tag{27}$$

$$\phi_\infty - \phi_2 = K_U h_2^{p_L} \tag{28}$$

Equations (27) and (28) represent a system of two equations with two unknowns, K_U and ϕ_∞ . In these equations, the numerical solutions ϕ_1 and ϕ_2 are known, as are the values of h_1 and h_2 ; and it is assumed that the asymptotic order (p_L) of the discretization error is known and that the value is equal to the asymptotic order of the truncation error. Solving Eqs. (27) and (28) to ϕ_∞ , one obtains the expression for the Richardson extrapolation given in Eq. (21), concluding its deduction.

Deduction of the Richardson Extrapolation with Apparent Order

The apparent order (p_U) is defined as the local slope on a curve of numerical solution uncertainty versus the grid spacing in a logarithmic graph. Its value allows one to verify in practice whether the asymptotic order (p_L) is achieved as $h \rightarrow 0$. Mathematically, the apparent order (p_U) is obtained [19] from

$$U(\phi) = K_U h^{p_U} \tag{29}$$

where K_U is a coefficient which is assumed to be independent of h . Introducing Eq. (2) into (29), one has

$$\phi_\infty - \phi = K_U h^{p_U} \tag{30}$$

With Eq. (30) applied to three different grids, h_1 , h_2 , and h_3 , whose numerical solutions are ϕ_1 , ϕ_2 , and ϕ_3 , respectively, one gets

$$\left. \begin{aligned} \phi_\infty - \phi_1 &= K_U h_1^{p_U} \\ \phi_\infty - \phi_2 &= K_U h_2^{p_U} \\ \phi_\infty - \phi_3 &= K_U h_3^{p_U} \end{aligned} \right\} \quad (31)$$

where the unknowns of this equation system are ϕ_∞ , K_U , and p_U . Solving this system, one obtains

$$p_U = \frac{\log [(\phi_2 - \phi_3)/(\phi_1 - \phi_2)]}{\log(q)} \quad (32)$$

$$\phi_\infty = \phi_1 + \frac{(\phi_1 - \phi_2)}{(q^{p_U} - 1)} \quad (33)$$

where the grid refinement ratio (q) is given in Eq. (22) and is assumed to be constant among grids h_1 , h_2 , and h_3 . The value of p_U represents an averaged slope of the uncertainties U_1 , U_2 , and U_3 between h_1 and h_3 on a U -versus- h logarithmic graph. The expression for ϕ_∞ given in Eq. (33) is the Richardson extrapolation already shown in Eq. (21). The differences are only p_L and p_U . With Eq. (33) into (20), one has

$$U_{Ri}(\phi_1) = \frac{(\phi_1 - \phi_2)}{(q^{p_U} - 1)} \quad (34)$$

In Eqs. (21) and (23), it was assumed that the discretization error asymptotic order was equal to the truncation error asymptotic order. This assumption was neglected in Eqs. (33) and (34). In this case, the order is obtained in function of numerical solutions, Eq. (32), that is, its value is unknown *a priori*. So, in principle, p_U can be calculated for any problem and variable of interest. The same is valid for ϕ_∞ and U_{Ri} calculated with Eqs. (33) and (34).

The apparent order (p_U) is only equal to asymptotic order (p_L) on any h if Eq. (19), for the discretization error, is constituted by a single term. That can be verified by comparing Eq. (19) to (29). However, generally, there are several or infinite terms in Eq. (19) as $h \neq 0$. So, in general, p_U is different from p_L and it can assume larger or smaller values than p_L , negative values, or otherwise nonexistent values due to the negative argument of the logarithm in Eq. (32). However, for $h \rightarrow 0$, $p_U \rightarrow p_L$ because the first term of the error is the leading term.

The Richardson Series

The constraints in using Richardson extrapolation can be better understood through the Richardson series, whose concept is introduced in this work as follows. It can be shown from Eqs. (24) and (2) that

$$\phi_\infty = \phi_1 + R_\infty(\phi_1 - \phi_2) \quad (35)$$

where

$$R_\infty = \frac{1}{\Psi} + \frac{1}{\Psi^2} + \frac{1}{\Psi^3} + \frac{1}{\Psi^4} + \dots \tag{36}$$

$$\Psi = q^p \tag{37}$$

The parameter Ψ is called the convergence ratio and R_∞ is the Richardson series, which is a geometric progression. If $\Psi < -1$ or $\Psi > 1$, this series converges toward finite values given by

$$R_\infty = \frac{1}{(\Psi - 1)} \tag{38}$$

Introducing Eqs. (37) and (38) into (35), one obtains the Richardson extrapolation, Eq. (21) or (33). So, it can be understood as the sum of an infinite number of terms in a geometric progression in which q and p are constant between h_2 (coarse grid) and h_1 (fine grid) down to $h = 0$, and $\Psi < -1$ or $\Psi > 1$.

Table 5 summarizes the values assumed by the apparent order (p_U) and by R_∞ as functions of four intervals for the values of Ψ . From this table, one verifies that only positive apparent order values must be employed in the Richardson extrapolation, that is $p_U > 0$, because in this case the Richardson series converges toward a finite value. On the contrary, Celik and Karatekin [20] propose, in the intervals, II, III, and IV of Ψ , the Richardson extrapolation may not be used either because the Richardson series diverges or because p_U does not exist. The same things are applied to the Richardson error estimator since, from Eqs. (20), (35), (37), and (38), one obtains

$$\frac{U_{Ri}}{(\phi_1 - \phi_2)} = R_\infty = \frac{1}{(q^p - 1)} \tag{39}$$

CONVERGENT APPARENT ORDERS

For all 10 cases in Table 1 and for the four numerical variables of interest in Table 2, it can be verified that the apparent order (p_U) converges monotonically to the asymptotic order (p_L) of the numerical solution error as $h \rightarrow 0$. This happens in two ways that are defined as subconvergent and superconvergent intervals of the apparent order, whose concepts are introduced in this work as follows.

Table 5. Values of the apparent order (p_U) as functions of the convergence ratio (Ψ)

Interval	Ψ	p_U	R_∞
I	$\Psi > 1$	$p_U > 0$	Finite
II	$0 < \Psi \leq 1$	$p_U \leq 0$	Infinite
III	$-1 \leq \Psi < 0$	Undefined	Infinite
IV	$\Psi < -1$	Undefined	Finite

Subconvergent Interval of the Apparent Order

Within the subconvergent interval, p_U converges monotonically to p_L with smaller values than p_L . This is illustrated in Figure 3. The subconvergent interval is defined as the interval $0 \leq h \leq h_C$, where $p_U(h)$ is positive, increasing with $h \rightarrow 0$, and smaller than or equal to p_L , that is,

$$0 < p_U(h_C) \leq p_U(h) \leq p_L \quad (0 \leq h \leq h_C) \tag{40}$$

$$\frac{dp_U}{dh} \leq 0 \quad (0 \leq h \leq h_C) \tag{41}$$

where h_C is the maximum value of h in the subconvergent interval, that is, it is the maximum value of h up to which Eqs. (40) and (41) are valid; and p_U is decreasing as h is increased.

Superconvergent Interval of the Apparent Order

Within the superconvergent interval, p_U converges monotonically to p_L with larger values than p_L . This is illustrated in Figure 4. The superconvergent interval is defined as the interval $0 \leq h \leq h_C$, where $p_U(h)$ is positive, decreasing with $h \rightarrow 0$, and larger or equal to p_L , that is,

$$0 < p_L \leq p_U(h) \leq p_U(h_C) \quad (0 < h \leq h_C) \tag{42}$$

$$\frac{dp_U}{dh} \geq 0 \quad (0 \leq h \leq h_C) \tag{43}$$

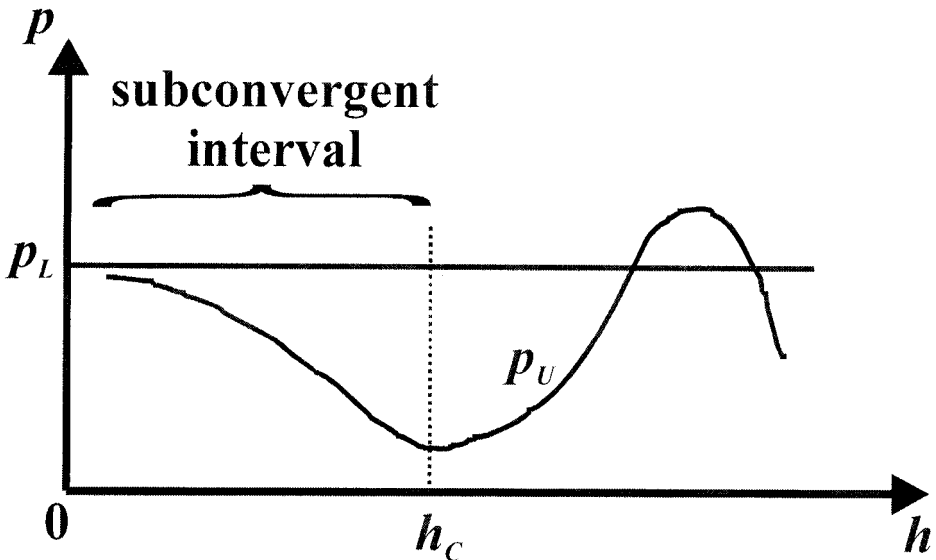


Figure 3. Definition of subconvergent interval of the apparent order.

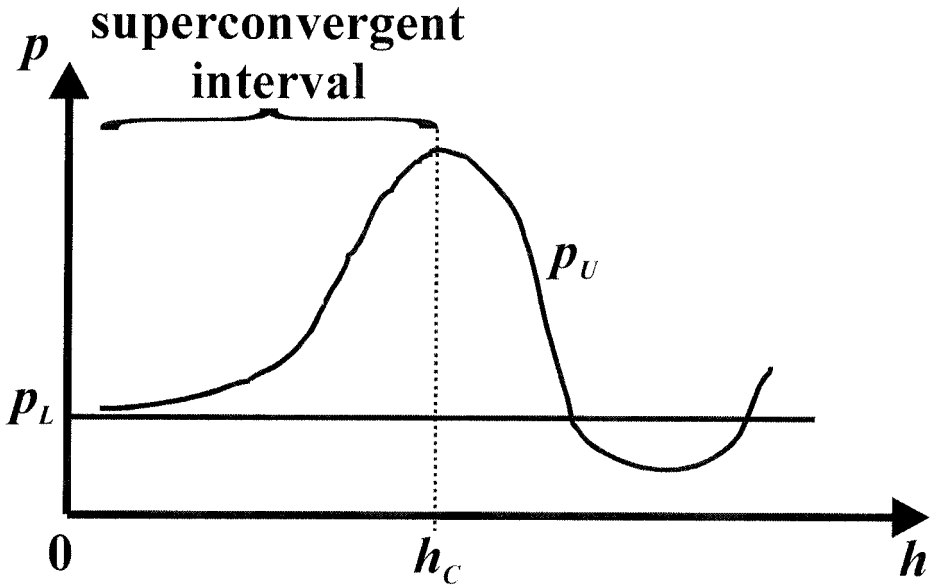


Figure 4. Definition of superconvergent interval of the apparent order.

where h_C is the maximum value of h in the superconvergent interval, that is, it is the maximum value of h up to which Eqs. (42) and (43) are valid; and p_U is increasing as h is increased.

Remarks and Example

One supposes that all numerical solutions of every variable of interest generate curves of p_U versus h which are either subconvergent or superconvergent as $h \rightarrow 0$. The types of curves of p_U versus h which are possible to obtain can be either as simple as those illustrated in Figures 3 and 4 or more complex, like that shown in Figure 5. In this figure p_U is positive, but it is also negative or undefined.

The example in Figure 5 refers to case 7 in Table 1 for the numerical variable λ_{DDS-2}^i obtained by Eq. (15) at $x = 0$ and with $q = 2$. It can be noticed in this figure that: at $h = 0.125$, p_U is larger than p_L , whose value is 2; at $h = 0.0625$, p_U is undefined due to the negative argument of the logarithm in Eq. (32), but it was plotted with value zero in Figure 5; at $h = 0.03125$, p_U is negative; and at smaller values than $h = 0.03125$ p_U is subconvergent. These values of p_U that match with the four larger values of h in Figure 5 exemplify the four types of apparent order values which can be obtained. One notes in Figure 5 that $p_U \rightarrow 2$ as $h \rightarrow 0$, that is, $p_L = 2$. This result is equal to the asymptotic order of the truncation error of the numerical approximation λ_{DDS-2}^i shown in Table 4.

The maximum value of h which defines a convergent interval, that is, h_C , depends on the mathematical and numerical models employed to obtain the numerical solutions. However, in any case, h_C defines the point up to which the first term in the discretization error equation (E), Eq. (19), is the leading term. In the present work, a procedure was not found to estimate *a priori* the value of h_C , that is,

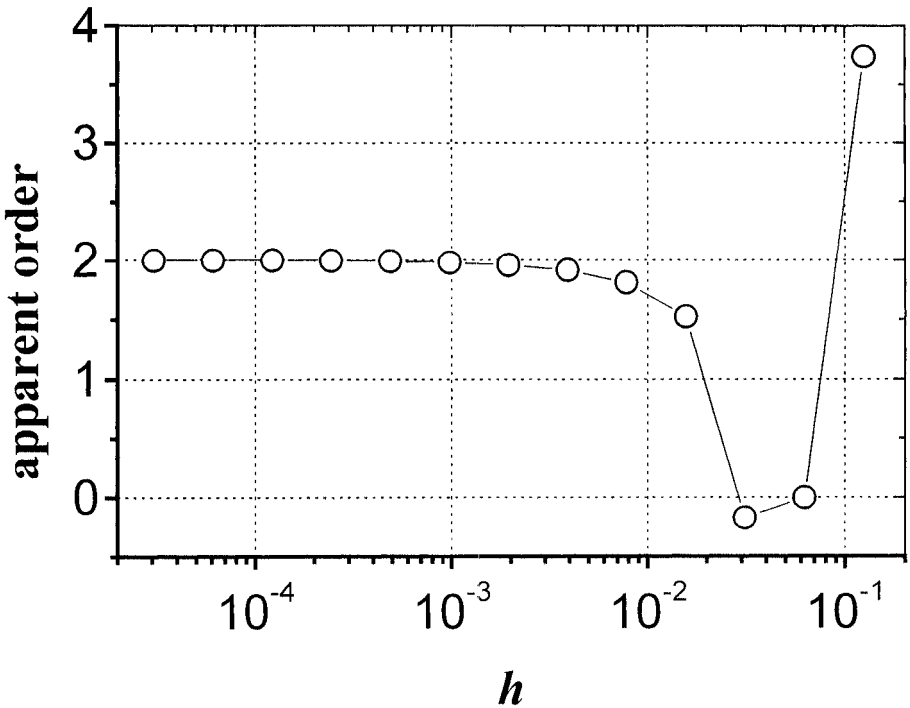


Figure 5. Example of expected values for the apparent order.

a procedure which showed when a value of apparent order is within of the convergent interval for any h given except when one obtains curves like that in Figure 5.

For the particular case of $p_U = p_L$ in any h , by definition, p_U is subconvergent and superconvergent simultaneously or, simply, converged. One can show [25] that: (1) if Eq. (19) has two or more terms and the first two terms have opposite signs, then p_U is subconvergent as $h \rightarrow 0$; and (2) if Eq. (19) has two or more terms with same sign, then p_U is superconvergent.

BOUNDS FOR ANALYTICAL SOLUTIONS AND ERRORS

Deduction of Bounds for the Discretization Error

In the following, we show that the Richardson error estimator allows us to calculate two values of uncertainty (U_{Ri}) which bound the discretization error when the apparent order (p_U) is convergent. So, one can obtain a value of uncertainty which is reliable certainly, that is, $U/E \geq 1$. With the Richardson error estimator and three numerical solutions (ϕ_1, ϕ_2 , and ϕ_3) obtained on three grids (h_1, h_2 , and h_3), it is possible to calculate uncertainties (U_{Ri}) using the asymptotic order (p_L), Eq. (23), and the apparent order (p_U), Eq. (34). Hereafter, these two uncertainties are denoted as $U_{Ri}(p_L)$ and $U_{Ri}(p_U)$, respectively.

The uncertainties calculated with Eqs. (23) and (34) refer to the numerical solution ϕ_1 obtained on the grid h_1 . From Eqs. (39), (36), and (37) for p_L , one gets

$$\frac{U_{\text{Ri}}(p_L)}{(\phi_1 - \phi_2)} = R_\infty(p_L) = \frac{1}{q^{p_L}} + \frac{1}{q^{p_L+p_L}} + \frac{1}{q^{p_L+p_L+p_L}} + \cdots = \frac{1}{(q^{p_L} - 1)} \quad (44)$$

It is implicit in this equation that p_L is constant between h_2 and $h \rightarrow 0$, in accordance with Eqs. (25) and (26). This assumption is right when the types of numerical approximations used in numerical models are kept constant. For example, in Table 4 for λ_{UDS}^i , $p_L = 1$ and for λ_{CDS}^i , $p_L = 2$. However, p_L is only reached at $h = 0$.

From Eqs. (39), (36), and (37) for p_U , one obtains

$$\frac{U_{\text{Ri}}(p_U)}{(\phi_1 - \phi_2)} = R_\infty(p_U) = \frac{1}{q^{p_U}} + \frac{1}{q^{p_U+p_U}} + \frac{1}{q^{p_U+p_U+p_U}} + \cdots = \frac{1}{(q^{p_U} - 1)} \quad (45)$$

It is implicit in this equation that p_U is constant between h_3 and $h \rightarrow 0$, in accordance with Eq. (31). Generally, this assumption is wrong because in practice, even within a convergent interval, p_U is a function of h , that is, at h_1 one has $p_U(h_1)$, which changes monotonically to reach p_L at $h = 0$. This can be seen, for example, in Figure 5. Therefore, for p_U convergent, from Eqs. (39), (36), and (37) for a real case, it follows that

$$\frac{E}{(\phi_1 - \phi_2)} = R_\infty(p_M) = \frac{1}{q^{p_a}} + \frac{1}{q^{p_a+p_b}} + \frac{1}{q^{p_a+p_b+p_c}} + \cdots = \frac{1}{(q^{p_M} - 1)} \quad (46)$$

where p_a, p_b, p_c , etc., are between p_L and $p_U(h_1)$ as p_U is convergent; p_a represents the curve of p_U between h_1 and h_a ; p_b represents the curve of p_U between h_a and h_b ; p_c represents the curve of p_U between h_b and h_c ; and so on; h_a, h_b, h_c , etc., represent successively more refined grids than h_1 ; and the order p_M represents a mean value of p_U between h_1 and $h = 0$.

With Eqs. (44) and (46), one gets

$$\frac{U_{\text{Ri}}(p_L)}{E} = \frac{R_\infty(p_L)}{R_\infty(p_M)} = \frac{(1/q^{p_L}) + (1/q^{p_L+p_L}) + (1/q^{p_L+p_L+p_L}) + \cdots}{(1/q^{p_a}) + (1/q^{p_a+p_b}) + (1/q^{p_a+p_b+p_c}) + \cdots} = \frac{(q^{p_M} - 1)}{(q^{p_L} - 1)} \quad (47)$$

and with Eqs. (45) and (46),

$$\frac{U_{\text{Ri}}(p_U)}{E} = \frac{R_\infty(p_U)}{R_\infty(p_M)} = \frac{(1/q^{p_U}) + (1/q^{p_U+p_U}) + (1/q^{p_U+p_U+p_U}) + \cdots}{(1/q^{p_a}) + (1/q^{p_a+p_b}) + (1/q^{p_a+p_b+p_c}) + \cdots} = \frac{(q^{p_M} - 1)}{(q^{p_U} - 1)} \quad (48)$$

Remembering that the grid refinement ratio (q) is always larger than the unity, if $p_U(h_1)$ is subconvergent, this means that

$$p_U(h_1) < p_a < p_b < p_c < \cdots < p_L \quad (49)$$

So, from Eqs. (47) and (48), one obtains

$$\frac{U_{\text{Ri}}(p_L)}{E} \leq 1 \leq \frac{U_{\text{Ri}}(p_U)}{E} \quad (\text{if } p_U \text{ is subconvergent}) \quad (50)$$

In other words, $U_{\text{Ri}}(p_L)$ and $U_{\text{Ri}}(p_U)$ bound the discretization error (E) of the numerical solution (ϕ_1) when p_U is subconvergent. If $p_U(h_1)$ is superconvergent, this means that

$$p_U(h_1) > p_a > p_b > p_c > \dots > p_L \tag{51}$$

So, from Eqs. (47) and (48), one has

$$\frac{U_{Ri}(p_U)}{E} \leq 1 \leq \frac{U_{Ri}(p_L)}{E} \quad (\text{if } p_U \text{ is superconvergent}) \tag{52}$$

Therefore, $U_{Ri}(p_L)$ and $U_{Ri}(p_U)$ again bound the discretization error (E) of the numerical solution (ϕ_1) when p_U is superconvergent.

With Eqs. (50) and (52), it can be concluded that the discretization error (E) is bounded by uncertainties $U_{Ri}(p_L)$ and $U_{Ri}(p_U)$ as p_U is convergent. In other words, $U_{Ri}(p_L)$ and $U_{Ri}(p_U)$ represent lower and upper bounds for E . So, these equations allow one to calculate reliable uncertainties, that is, $U/E \geq 1$. Thus, if p_U is subconvergent, $U_{Ri}(p_U)$ is reliable as Eq. (50), and if p_U is superconvergent, $U_{Ri}(p_L)$ is reliable as Eq. (52). From Eqs. (47) and (48), it is verified that when the value of p_U approaches to the value of p_L , the ratios $U_{Ri}(p_L)/E$ and $U_{Ri}(p_U)/E$ approach to the unity and therefore the error estimates are more accurate.

Exact Analytical Solution Bounds

Expressions have been obtained to calculate the estimated analytical solution (ϕ_∞) with asymptotic order (p_L), Eq. (21), and with apparent order (p_U), Eq. (33). Hereafter, these two values of ϕ_∞ are denoted as $\phi_\infty(p_L)$ and $\phi_\infty(p_U)$, respectively. From Eqs. (47) and (48), it is possible to show that

$$\frac{\phi_\infty(p_L)}{\Phi} \leq 1 \leq \frac{\phi_\infty(p_U)}{\Phi} \quad (\text{if } p_U \text{ is subconvergent}) \tag{53}$$

$$\frac{\phi_\infty(p_U)}{\Phi} \leq 1 \leq \frac{\phi_\infty(p_L)}{\Phi} \quad (\text{if } p_U \text{ is superconvergent}) \tag{54}$$

In other words, $\phi_\infty(p_L)$ and $\phi_\infty(p_U)$ bound the exact analytical solution (Φ) when p_U is convergent, and they represent lower and upper bounds for Φ .

Here also, when the value of p_U approaches to the value of p_L , the ratios $\phi_\infty(p_L)/\Phi$ and $\phi_\infty(p_U)/\Phi$ approach to the unity. The signs of equality employed in Eqs. (50), (52), (53), and (54) are only applied to the limit case where the discretization error equation, Eq. (19), has a single term, that is, when $p_U = p_L$ at any h .

Figure 6 illustrates the bounds for the exact analytical solution, Eq. (53), and for the discretization error, Eq. (50), when p_U is subconvergent. In this figure can be noted the numerical solutions ϕ_1 and ϕ_2 obtained on grids h_1 and h_2 , the exact analytical solution Φ , $\phi_\infty(p_L)$, $\phi_\infty(p_U)$, the discretization error of ϕ_1 , $E(\phi_1)$, obtained from Eq. (1), $U_{Ri}(p_L)$ and $U_{Ri}(p_U)$.

THE CONVERGENT ERROR ESTIMATOR

As shown in Figure 6, it was seen in the previous section that the exact analytical solution (Φ) of a variable of interest is bounded by $\phi_\infty(p_L)$ and $\phi_\infty(p_U)$ when the apparent order (p_U) is convergent. Based on this, the convergent numerical solution (ϕ_c) can be defined as an average of the values $\phi_\infty(p_L)$ and $\phi_\infty(p_U)$, that is,

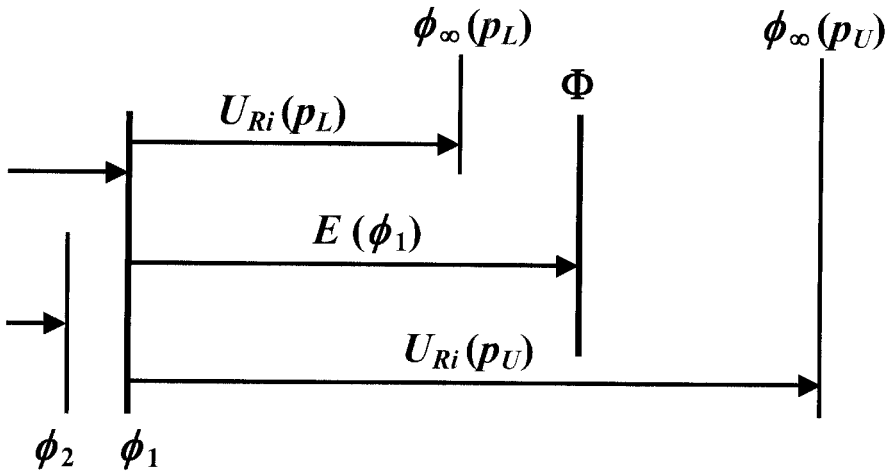


Figure 6. Bounds for the exact analytical solution (Φ) and for the discretization error (E) when p_U is subconvergent.

$$\phi_C = \frac{[\phi_\infty(p_L) + \phi_\infty(p_U)]}{2} \tag{55}$$

where $\phi_\infty(p_L)$ and $\phi_\infty(p_U)$ are obtained by the Richardson extrapolation, Eqs. (21) and (33), respectively. The uncertainty of ϕ_C is equal to the modulus of half of the interval between $\phi_\infty(p_L)$ and $\phi_\infty(p_U)$, that is,

$$U_C = \frac{|\phi_\infty(p_L) - \phi_\infty(p_U)|}{2} \tag{56}$$

To use ϕ_C and U_C , a suitable representation of a numerical solution (ϕ) is

$$\phi = \phi_C \pm U_C \tag{57}$$

For the case of subconvergent apparent order (p_U), Figure 7 illustrates the convergent numerical solution (ϕ_C), its respective uncertainty (U_C), as well as its discretization error (E_C). The other symbols are the same as those of Figure 6.

According to Eq. (55), ϕ_C is based on two extrapolated numerical solutions. One can show [25] that the asymptotic order of its error (E_C) is larger than the asymptotic order of the error of the numerical solutions (ϕ_1, ϕ_2 , and ϕ_3) used to calculate $\phi_\infty(p_L)$ and $\phi_\infty(p_U)$, and is equal to the second true order of the discretization error equation, Eq. (19), that is, it is equal to p_2 .

RESULTS

The 10 cases defined in Table 1 were solved by the finite-difference method [6] for the four numerical variables of interest in Table 2. We employed the six types of numerical approximations in Table 3, grid refinement ratio $q = 2$, and grid spacing $h = 0.5, 0.25, 0.125, \dots, 1.53 \times 10^{-5}$, which correspond to grids with 2, 4, 8, ..., 65,536 elements.

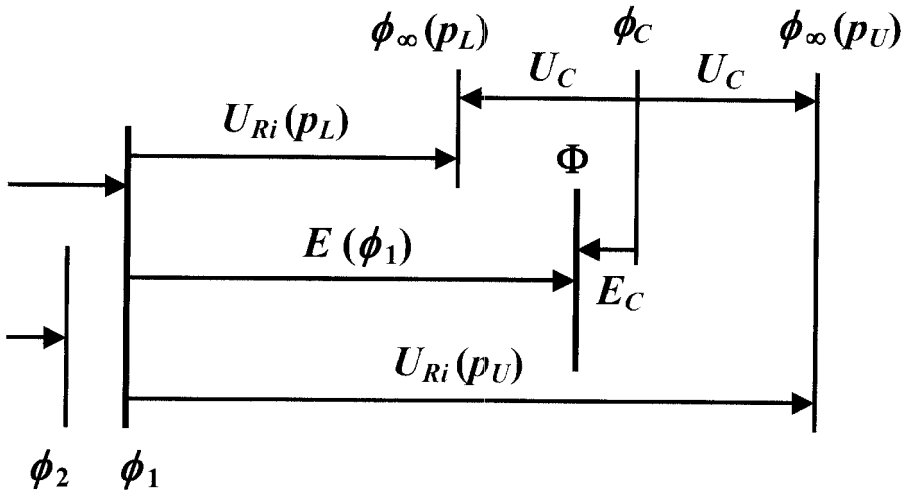


Figure 7. Example of a convergent numerical solution (ϕ_C) for subconvergent p_U .

Figures 5, 8, and 9 illustrate examples of the results obtained. This example refers to case 7 in Table 1 for the numerical variable $\lambda_{\text{DDS-2}}^i$, which was obtained by Eq. (15) at $x = 0$ and with $q = 2$. One can see in Figure 5 that the apparent order (p_U) is subconvergent for $h < 3.125 \times 10^{-2}$. So, for smaller values than this h ,

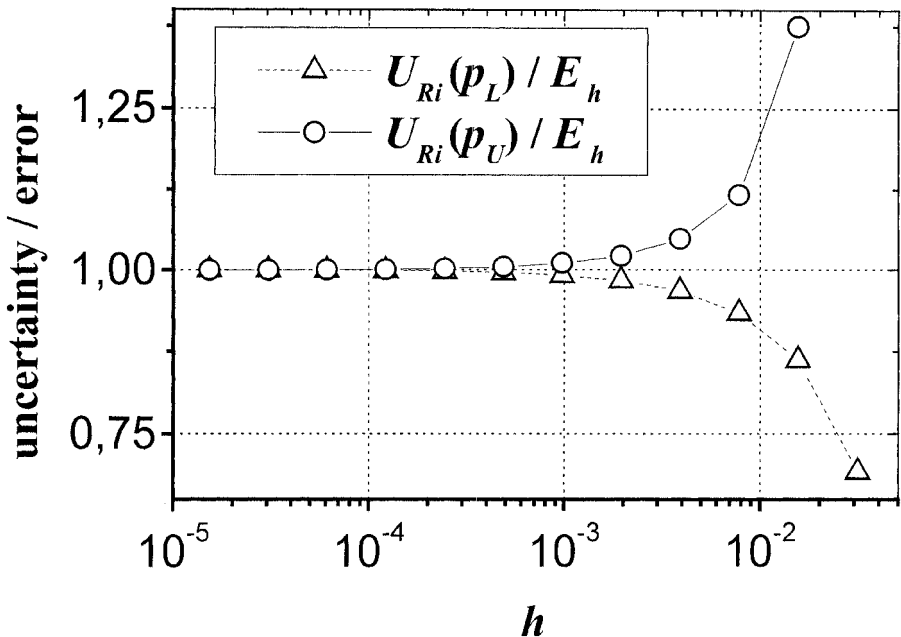


Figure 8. Ratio between uncertainty (U) and error (E) in the subconvergent interval of p_U for $\lambda_{\text{DDS-2}}^i$ of case 7.

modulus of uncertainties and errors

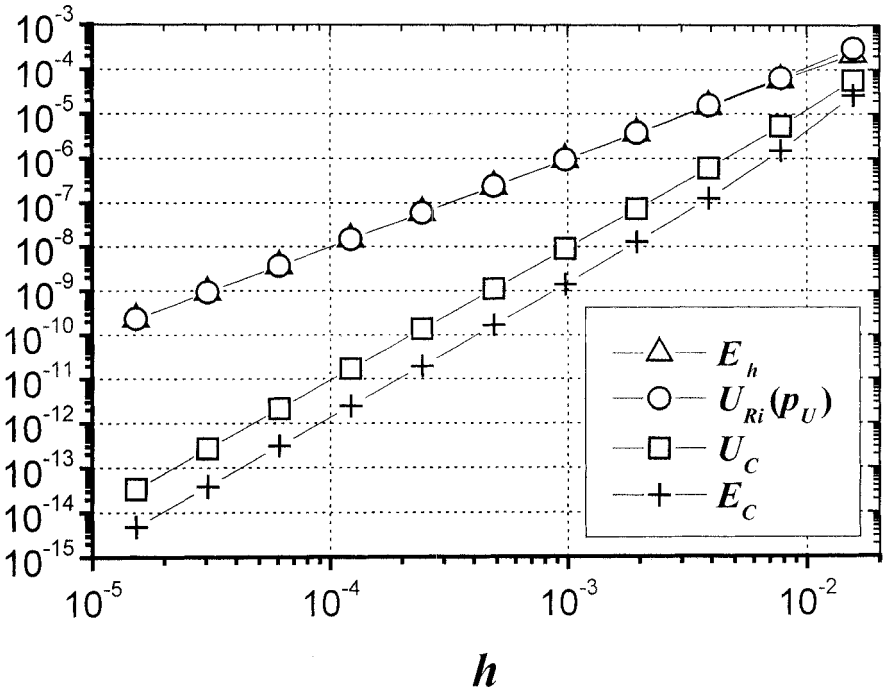


Figure 9. Modulus of errors and uncertainties for λ_{DDS-2}^i of case 7.

Eq. (50) is valid, as can be seen in Figure 8. In this example, $U_{Ri}(p_U)$ is the reliable uncertainty because its value is larger than the discretization error (E_h), and $U_{Ri}(p_L)$ is the lower bound of E_h .

In Figure 9 is shown the discretization error (E_h) of λ_{DDS-2}^i at $x = 0$, calculated by Eq. (1); the uncertainty $U_{Ri}(p_U)$ obtained with Eq. (34); the uncertainty (U_C) of the convergent numerical solution (ϕ_C), calculated by Eq. (56); and the error (E_C) of ϕ_C , obtained by the difference between the exact analytical solution of Λ^i and ϕ_C . In this figure, one can see that the value of U_C decreases a lot with respect to U_{Ri} as $h \rightarrow 0$. This happens by employing the same numerical results used to obtain U_{Ri} . The error asymptotic order of λ_{DDS-2}^i is $p_L = 2$, as shown in Table 4, but it is $p_L = 3$ for ϕ_C . This can be seen in Figure 9, where the slopes of E_C and U_C are larger than those of E_h and U_{Ri} . This increase of the error order of ϕ_C is shown in [25].

In Figure 5, it can be noted that $p_L \approx 2$ at $h \approx 0.09$. So, it is possible to obtain values of apparent order close to asymptotic order out of the convergent interval. This means that it is necessary to know when p_U is convergent in order to employ the Richardson error estimator reliably to calculate the uncertainty of a numerical solution. Therefore, error estimates based on only two or three numerical solutions, as in Eqs. (23) and (34), may not be considered reliable.

For all 10 cases in Table 1 and the four numerical variables of interest in Table 2, it was verified that the Richardson error estimator allows one to obtain accurate uncertainties (U_{Ri}) when grid spacing (h) vanishes, that is,

$$\frac{U_{Ri}}{E_h} \rightarrow 1 \quad \text{for } h \rightarrow 0 \quad (58)$$

where E_h is the discretization error calculated by Eq. (1). Equation (58) is valid for U_{Ri} obtained with either the asymptotic order (p_L) or the apparent order (p_U) by Eqs. (23) and (34), respectively.

CONCLUSION

The concept of a convergent interval for the uncertainty apparent order was introduced. Within this interval, we verified for all 10 cases and the four numerical variables of interest that:

1. The value of the apparent order (p_U) approaches the asymptotic order (p_L) monotonically.
2. According to Eqs. (50) and (52), the discretization error (E_h) is bounded between $U_{Ri}(p_L)$ and $U_{Ri}(p_U)$, whose values are calculated using the Richardson error estimator with p_L and p_U by Eqs. (23) and (34).
3. The accuracy of a discretization error estimate depends on the difference between p_U and p_L . When the value of p_U approaches to the value of p_L , the ratios $U_{Ri}(p_L)/E_h$ and $U_{Ri}(p_U)/E_h$ approach to the unity and so the error estimate is more accurate. As $h \rightarrow 0$, $U_{Ri}/E_h \rightarrow 1$, according to Eq. (58).
4. The exact analytical solution (Φ) is bounded between $\phi_\infty(p_L)$ and $\phi_\infty(p_U)$, whose values are calculated using the Richardson extrapolation with p_L and p_U by Eqs. (21) and (33).
5. A convergent numerical solution (ϕ_C) was defined which is based on $\phi_\infty(p_L)$ and $\phi_\infty(p_U)$. Its error (E_C) is smaller than E_h .

Outside convergent interval of p_U , there is not assurance about the five conclusions above. We did not find a procedure to estimate *a priori* the beginning of the convergent interval of p_U , denoted by h_C . In this work, h_C was obtained by calculation of p_U as a function of h as in Figure 5. Therefore, error estimates based on numerical solutions obtained over only two or three grids may not be considered reliable.

REFERENCES

1. E. Kreyszig, *Advanced Engineering Mathematics*, 8th ed., Wiley, New York, 1999.
2. F. G. Blottner, Accurate Navier–Stokes Results for the Hypersonic Flow over a Spherical Nosedip, *J. Spacecraft Rockets*, vol. 27, pp. 113–122, 1990.
3. P. J. Roache, Perspective: A Method for Uniform Reporting of Grid Refinement Studies, *J. Fluids Eng.*, vol. 116, pp. 405–413, 1994.
4. P. J. Roache, *Verification and Validation in Computational Science and Engineering*, Hermosa, Albuquerque, NM, 1998.

5. U. B. Mehta, Guide to Credible Computer Simulations of Fluid Flows, *J. Propulsion Power*, vol. 12, pp. 940–948, 1996.
6. J. C. Tannehill, D. A. Anderson, and R. H. Pletcher, *Computational Fluid Mechanics and Heat Transfer*, 2nd ed., Taylor & Francis, Washington, DC, 1997.
7. W. L. Oberkampf and F. G. Blottner, Issues in Computational Fluid Dynamics Code Verification and Validation, *AIAA J.*, vol. 36, pp. 687–695, 1998.
8. AIAA, Guide for the Verification and Validation of Computational Fluid Dynamics Simulations, AIAA G-077-1998, American Institute of Aeronautics and Astronautics, Reston, VA, 1998.
9. A. Jameson and L. Martinelli, Mesh Refinement and Modeling Errors in Flow Simulation, *AIAA J.*, vol. 36, pp. 676–686, 1998.
10. A. Rizzi and J. Vos, Toward Establishing Credibility in Computational Fluid Dynamics Simulations, *AIAA J.*, vol. 36, pp. 668–675, 1998.
11. J. H. Ferziger and M. Peric, *Computational Methods for Fluid Dynamics*, 2nd ed., Springer-Verlag, Berlin, 1999.
12. W. S. Dorn and D. D. McCracken, *Numerical Methods with Fortran IV Case Studies*, Wiley, New York, 1972.
13. R. W. Hamming, *Numerical Methods for Scientists and Engineers*, 2nd ed., Dover, New York, 1973.
14. J. Z. Zhu and O. C. Zienkiewicz, Superconvergence Recovery Technique and *a Posteriori* Error Estimates, *Int. J. Numer. Meth. Eng.*, vol. 30, pp. 1321–1339, 1990.
15. M. Ainsworth and J. T. Oden, *a Posteriori* Error Estimation in Finite Element Analysis, *Comput. Meth. Appl. Mech. Eng.*, vol. 142, pp. 1–88, 1997.
16. L. Babuska, F. Ihlenburg, T. Strouboulis, and S. K. A. Gangaraj, *a Posteriori* Error Estimation for Finite Element Solutions of Helmholtz' Equation, Part I: The Quality of Local Indicators and Estimators, *Int. J. Numer. Meth. Eng.*, vol. 40, pp. 3443–3462, 1997.
17. M. Hortmann, M. Peric, and G. Scheuerer, Finite Volume Multigrid Prediction of Laminar Natural Convection: Bench-Mark Solutions, *Int. J. Numer. Meth. Fluids*, vol. 11, pp. 189–207, 1990.
18. L. F. Richardson and J. A. Gaunt, The Deferred Approach to the Limit, *Phil. Trans. R. Soc. Lond. Ser. A*, vol. 226, pp. 299–361, 1927.
19. G. de Vahl Davis, Natural Convection of Air in a Square Cavity: A Bench Mark Numerical Solution, *Int. J. Numer. Meth. Fluids*, vol. 3, pp. 249–264, 1983.
20. I. Celik and O. Karatekin, Numerical Experiments on Application of Richardson Extrapolation with Nonuniform Grids, *J. Fluids Eng.*, vol. 119, pp. 584–590, 1997.
21. B. Szabò and I. Babuska, *Finite Element Analysis*, Wiley, New York, 1991.
22. C. A. J. Fletcher, *Computational Techniques for Fluid Dynamics*, 2nd ed., Springer-Verlag, Berlin, 1997.
23. R. H. Pletcher, W. J. Minkowycz, E. M. Sparrow, and G. E. Schneider, Overview of Basic Numerical Methods, in W. J. Minkowycz, E. M. Sparrow, G. E. Schneider, and R. H. Pletcher (eds.), *Handbook of Numerical Heat Transfer*, Chap. 1, Wiley, New York, 1988.
24. L. F. Richardson, The Approximate Arithmetical Solution by Finite Differences of Physical Problems Involving Differential Equations, with an Application to the Stresses in a Masonry Dam, *Phil. Trans. R. Soc. Lond. Ser. A*, vol. 210, pp. 307–357, 1910.
25. C. H. Marchi, Verification of Unidimensional Numerical Solutions in Fluid Dynamics (in Portuguese, Verificação de Soluções Numéricas Unidimensionais em Dinâmica dos Fluidos), Ph.D. thesis, Federal University of Santa Catarina, Florianópolis, Brazil, 2001.